



Tomographic Investigation of Plasma Jets Produced by Multielectrode Plasma Torches

J. Schein, M. Richter, K. D. Landes, G. Forster, J. Zierhut, and M. Dzulko

(Submitted September 7, 2007; in revised form April 30, 2008)

Recent advances in the development of new plasma torches rely on the use of multiple electrodes to improve plasma jet stability. Examples are the Triplex, employing three cathodes and a single anode, and the Delta, which uses three anodes with a single common cathode. To characterize the plasma jet produced by these plasma torches, initial experiments have been performed using tomography in the visible range. Due to the improved stability of the plasma jet in the multielectrode configuration it is possible to carry out tomography by means of a regular charge-coupled device (CCD) camera, which is rotated around the plasma jet axis. The two-dimensional information obtained by the CCD camera is subsequently processed to produce an image of the three-dimensional emission distribution. The tomographic analysis is mated with a simple but effective simulation tool, which can be used as a basis for parameter-dependent multielectrode plasma torch design.

Keywords diagnostics and control, multielectrode plasma torches, plasma jet shape, stability of TS process, TS coating process, three-dimensional optical measurement

1. Introduction

In plasma spray systems, the most important characteristic from the industrial viewpoint is the quality of the coating and the speed and efficiency of deposition. This, however, is determined by how quickly and how homogeneously the particles injected into a plasma jet are heated, which in turn depends on the “quality” of the jet itself. A long and, most importantly, stable jet is best suited for this task. Single-anode, single-cathode plasma torches such as the Sulzer Metco F4 torch (Westbury, NY), the workhorse of plasma spraying for decades, show significant fluctuations of plasma jet length (Ref 1, 2) due to the requirement of constant movement of the anode attachment, which is needed to prevent the occurrence of preferred arc attachment points and erosion. The fluctuations of jet length in turn affect the residency time of the particles in the jet, leading to variations in particle temperature thus limiting the reproducibility and obtainable quality of the coating. To circumvent these problems, approaches with multiple torches (e.g., triple torch) (Ref 3) have been made, which produce a more homogenous heating environment.

Recent advances in the field of innovative plasma spray torches improve upon this principle by using multiple arcs

in a single torch. This approach is based on creating multiple stationary anode attachment and thus a stable plasma jet at a total energy input power similar to those used in single anode attachment torches. However, through the use of multiple arcs, the resulting plasma jet is no longer rotationally symmetric, which means that conventional diagnostic methods, relying on the validity of an Abel inversion (Ref 4), cannot be used to characterize the jet, thus leading to a lack of information with respect to the material processing qualities of the new torches. To overcome this problem, a new tool has been developed employing tomography, which has been validated using the Triplex torch and Delta gun (Fig. 1 and 2, respectively)—two examples of multielectrode plasma torches with separate anode attachments. These plasma sources offer, compared to single-arc systems, a more stationary plasma jet because the movement of the anode attachments is significantly limited: Axial movement is prevented by the implementation of an electrically isolated area between the cathode and the anode region, and rotational movement is reduced due to either physically separated anode pieces (Delta) or due to the eccentric position of the multiple cathodes (Triplex). The azimuthal motion along the anode is accompanied by a pronounced voltage increase that reduces such motion. To prevent erosion, the anode current is reduced by producing three anode attachment points. In the case of the Triplex (Fig. 1) (Ref 5-7), the plasma jet is generated by three individual arcs produced by three cathodes and a single ring-shaped anode. As described in Steenbeck’s minimum principle, the arc tends to reduce its length by choosing an anode attachment spot closest to the cathode, which leads to three different anode spots, hence, three individual arcs. Nevertheless, care has to be taken to properly design the nozzle diameter as, because of the self-magnetic field, these arcs will fuse if the nozzle region chosen is too small. The anode attachments still have an azimuthal degree of freedom, which depends on parameters such as plasma

J. Schein, M. Richter, K. D. Landes, G. Forster, J. Zierhut, and M. Dzulko, Universität der Bundeswehr, EIT, Munich, Germany. Contact e-mail: jochen.schein@unibw.de.

current and gas flow, and can therefore alter the shape of the plasma jet.

The Delta plasma torch (Ref 8) operates with three individual anodes and a common cathode. The common cathode produces a single arc that splits up close to the anode forced by the electric circuitry. While an azimuthal movement of the jet is not possible, the position of the arc breakup into three anodic “fingers” (A, Fig. 2) may shift along the plasma core axis, leading to an axial instability.

The triple anode attachment produces in Triplex and Delta torches a triangular structure of the plasma jet, which may enable a more efficient particle feed as a detailed knowledge of the jet structure can determine an optimum particle injection position. This is due to zones of high and low viscosity, which are present within the plasma jet and when identified provide a confined path toward the center of the jet, the so-called cage effect.

The triangular jet structure cannot be detected by simple lateral scan investigation. Therefore, the tomography measurement system is used to resolve three dimensions of

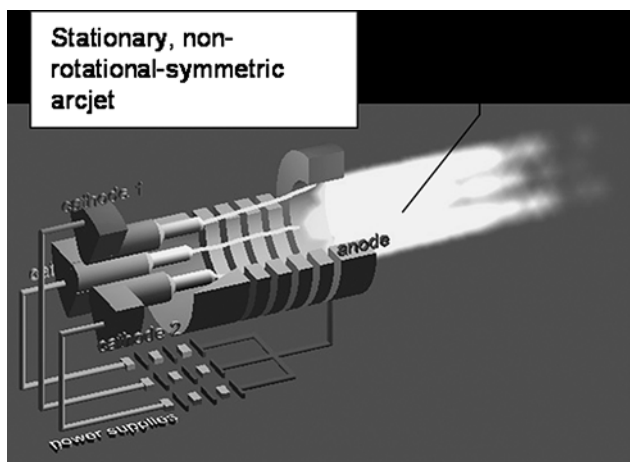


Fig. 1 Triplex plasma torch (Sulzer Metco) with three cathodes and a single ring anode

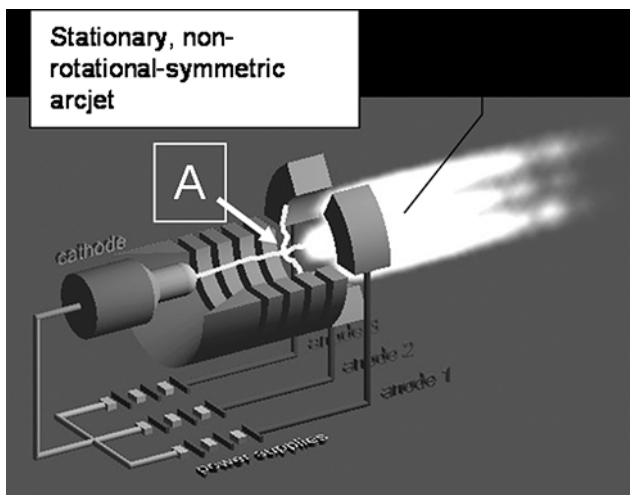


Fig. 2 Delta gun (GTV) with three anodes and a single cathode

the jets produced by Triplex and Delta plasma torches by looking at the radiation of the recombining plasma in two dimensions over an angle of 180° to reconstruct the three-dimensional (3D) structure of the jet.

2. Tomography

The measurement principle is shown in Fig. 3. A charge-coupled device (CCD) camera records the light of the plasma jet over an angle of 180° , covering a large fraction of the length of the jet (Ref 9, 10). Figure 4 shows the principle relationship between data collection and evaluation. The actual values of local emission cannot be measured directly; the data recorded are the integral of light emission in the direction of observation.

More precisely, let us assume the CCD chip has a resolution of $R \times S$ pixels (R , rows; S , columns) and that N images are taken at angular increments of $180/N$ degrees, that is, at angles $w \times N/180$, $w \in \{0, \dots, N - 1\}$. This setup leads to measurements of the emitted light along R parallel lines at N angular positions across S slices of the plasma jet.

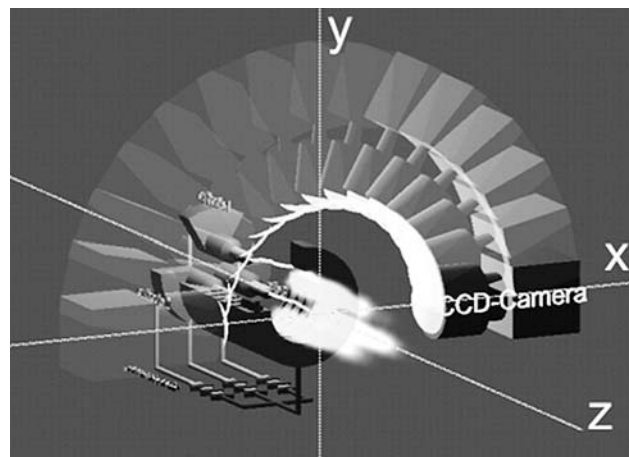


Fig. 3 Tomography, principle of measurement. A camera is rotated around the nonrotational symmetric plasma jet

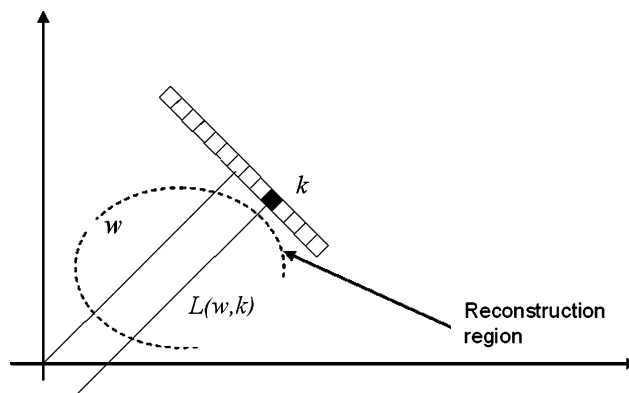


Fig. 4 Data acquisition using tomography, definition of variables

For a simplified mathematical model of the measurement, we consider a fixed cross section s of the plasma jet (corresponding to a fixed column of the CCD chip). Let w be the angular position and let $L(w, k)$, $k \in \{0, \dots, R-1\}$ be the straight line parallel to w , passing through the center of the k th pixel (in the s th column) of the CCD chip.

The measured intensity of emitted light now is modeled as:

$$M(w, k) = E \int_{L(w, k)} \varepsilon(x) dx \quad (\text{Eq 1})$$

where $\varepsilon(x)$ is the local emission in $x \in \mathbb{R}^2$ and where E is the sensitivity of the measurement system. Of course, the function ε is supported only in a bounded region (reconstruction region). Figure 4 illustrates how measurements look. In this simplified model we do not consider light absorption, as we assume the plasma to be optically thin. For the moment, we do not consider finite detector width, either. We assume ideal conditions.

From the set of our measurements, the function ε has to be reconstructed. A conceptually very simple way to achieve this is via the so-called algebraic reconstruction technique (ART). ART relies on a discretization of the function ε by decomposing it into pixels, i.e. by covering the reconstruction region by small squares Q_m , $m=0, \dots, M-1$, and assuming ε to be constant in each square. So we replace ε by a vector $u \in \mathbb{R}^M$ whose m th component is the value of ε in Q_m .

For easier notation we assemble our double index (w, k) into a single index $j=j(w, k)$ from now on, with $j=0, \dots, J-1, J=NR$. The lines of integration are accordingly designated L_j , and our measurements are denoted by M_j .

Now let:

$$a_{j,m} = \text{length}(L_j \cap Q_m)$$

and set

$$a_j = (a_{j,0}, \dots, a_{j,M-1})^T$$

Then Eq 1 can be written as:

$$a_j^T u = M_j, \quad j = 0, \dots, J-1 \quad (\text{Eq 2})$$

which is a set of J linear equations for the unknown coefficients $u \in \mathbb{R}^M$. We can write this system in closed form as:

$$Au = g \quad (\text{Eq 3})$$

where a_j^T is the j th row of matrix A and where M_j is the j th component of vector $g \in \mathbb{R}^J$. A typical example for the parameters involved is $R=N$ and $M=N^2$ for a resolution of $N \times N$ pixels in the reconstruction region. In this case, the linear system (Eq 3) is square, but even in this case it is unlikely to have a solution, because of discretization and measurement errors. Therefore, we can replace Eq 3 by a least squares problem, namely:

$$\min \|Au - g\|^2 \quad (\text{Eq 4})$$

which leads to the so-called normal equation:

$$A^T Au = A^T g \quad (\text{Eq 5})$$

In practice, systems such as Eq 3 or 5 are very large, but sparse, since every line L_j intersects only a small fraction of all pixels Q_m (\sqrt{M} , roughly). Such systems are best solved by iterative methods.

We chose the simultaneous iterative reconstruction technique (SIRT) for solving Eq 5. This will produce a sequence of approximations $u^{(k)}$, $k=0, 1, 2, \dots$ converging to u .

One step of the iteration reads

$$u^{(k+1)} = u^{(k)} + \omega SA^T (g - Au^{(k)})$$

where ω is a scalar relaxation parameter and where S is a diagonal matrix that is meant to normalize the columns of A^T such that the sum of elements in each column of SA^T becomes 1 (i.e., $S = \text{diag}(\sum_m a_{j,m})^{-1}$).

ART is quite versatile and allows for various generalizations and refinements:

- Other iterative methods are available for finding generalized solutions of Eq 3, such as the method of Kaczmarz (Ref 11).
- ε does not necessarily need to be approximated by piecewise constant functions. Polynomials, piecewise polynomials (splines), wavelets, and others can be used as well and may lead to better approximations of ε and possibly also to better convergence properties of ART.
- ART is applicable to more general situations than Eq 1. For example, the integration along lines may be replaced by one over areas, thus appropriately modeling finite detector width. Third, it is possible to incorporate the effects of absorption by multiplying matrix entries in Eq 3 by weighting factors.
- Equation 4 can be replaced by a more general optimization criterion that incorporates a priori information about the reconstruction region (leading to Bayesian estimates) (Ref 12).

3. Experimental Results

The CCD recording system consists of PCO Pixelfly VGA (Kehlheim, Germany) black-and-white camera with a resolution of 640×480 pixels, offering 12 bit dynamic range. For the experiments, an exposure time of 0.5 s was used to average fluctuations of the plasma.

The system is used to evaluate the described triple-arc systems. As the anode of a Triplex is a solid copper ring, covered by a tungsten layer, the anode attachments are not fixed, which enables movement of the attachments resulting in a change of the arc jet structure providing an interesting demonstration object for investigation. The characteristic angle, which is defined as the angle of rotation of the triangular jet structure in a single plane 2 cm outside the nozzle along the arc axis, is shown as

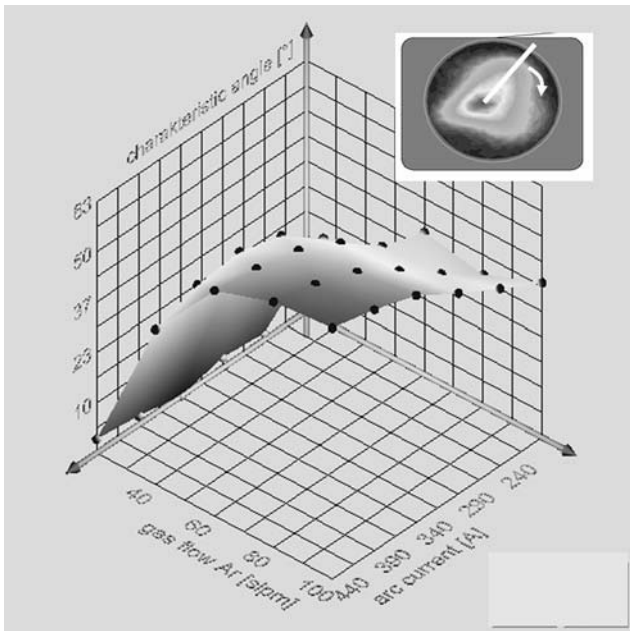


Fig. 5 Rotation of plasma jet (Triplex) as function of plasma current and gas flow. Small image indicates the characteristic angle

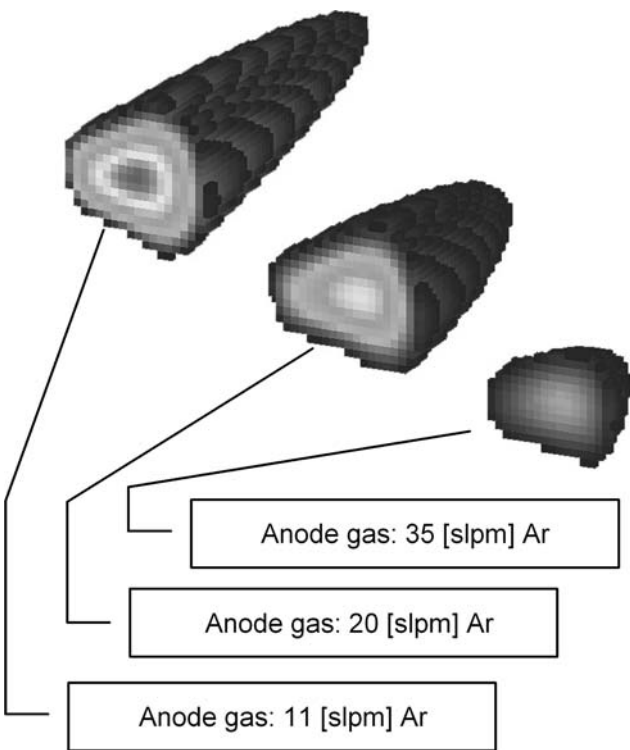


Fig. 6 Tomography results of plasma jet length. Delta gun with variable anode shroud cooling gas flow. Operational parameters: $I=163$ A, $P=10$ kW, plasma gas: Ar 15 sLpm

function of gas flow and arc current in Fig. 5. The tomography data show that the characteristic angle shifts (i.e., the jet rotates) with an increase of plasma gas flow

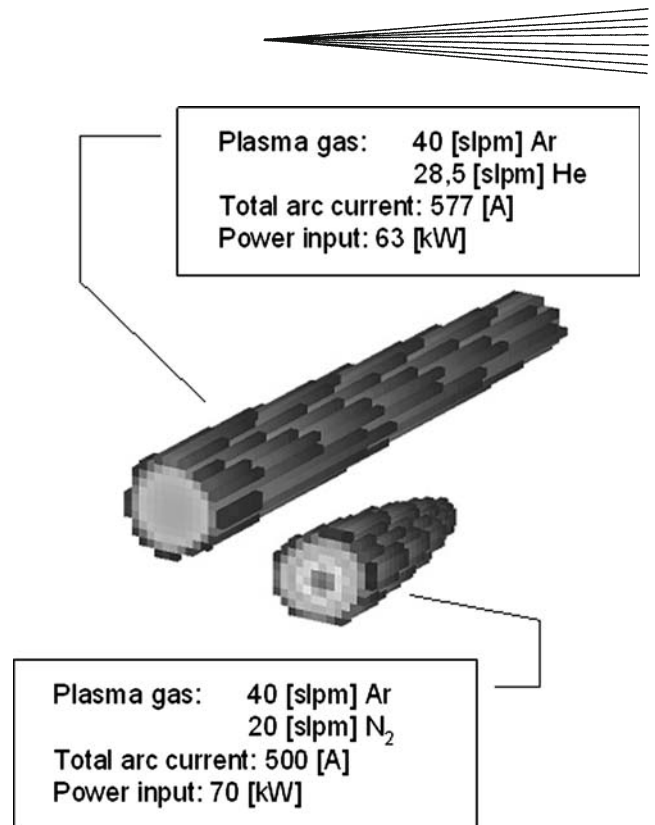


Fig. 7 Tomography results of plasma jet length. Delta gun operated with and without molecular gas. Operational parameters: $I=163$ A, $P=10$ kW, anode gas: Ar 20 sLpm

and plasma current. With tripling the gas flow, a shift of up to 60° was found for the Triplex II with 9 mm nozzle, which is most certainly caused by the vortex flow. A less pronounced relationship was found for the plasma current. While increasing plasma current also appears to change the characteristic angle, the increase seems to taper off at higher currents with a maximum rotation of approximately 10° only.

This rotation of the arc jet, which is most likely connected to a motion of the anode attachments, might lead to complications with the particle feed as the angle of injection may have to be changed for different plasma parameters (cage effect). More work is needed to quantify these changes and to implement the newfound parameters into a system control.

The Delta gun is certainly not subject to a change in anode root position, but in order to control the position and extend the lifetime of the electrodes an additional shroud gas flow around the anodes is necessary. The tomography system was used to determine the influence of this gas flow on the shape of the plasma jet. The results are summarized in Fig. 6. Even though the measurements are not spectrally resolved, the influence of the anode flow on jet length is obvious. The cold perpendicular flow reduces the arc jet length significantly.

Another investigation performed with the Delta gun to validate the tomography system was to demonstrate the influence of plasma gas composition on the plasma jet. From Fig. 7 the effect of introducing molecular gas is

clearly visible. The jet length is significantly reduced, and the gradient of light emission increased as expected, since the gas, through its dissociation, can store more energy at lower temperatures. Thus the total power injected into the jet leads to a lower maximum temperature and shorter jet length. Another reason is the increase in jet velocity with the addition of N_2 and thus the increased turbulence.

4. Emulation of Results

To enhance the possibilities of the tomography system, software was developed to emulate the acquired section images using two-dimensional analytic functions. As a first step a function $\tilde{\epsilon}$ was selected, a sum of three independent two-dimensional Gaussian profiles:

$$\tilde{\epsilon}(x, y) = \sum_{i=1}^3 A_i \cdot \left(e^{-\frac{1}{b_{1,i}} [\cos(\varphi_i) \cdot (x-x_{0,i}) - \sin(\varphi_i) \cdot (y-y_{0,i})]^2} \cdot e^{-\frac{1}{b_{2,i}} [\sin(\varphi_i) \cdot (x-x_{0,i}) + \cos(\varphi_i) \cdot (y-y_{0,i})]^2} \right)$$

A Gaussian profile is chosen because spectroscopic investigations to determine jet temperatures that used

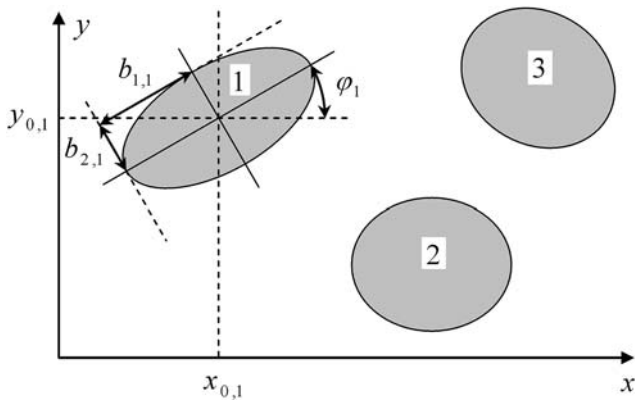


Fig. 8 Parameters of Gaussian profile for simulation

Gaussian profiles to perform Abel inversions have shown results that compared very well with measurement that did not assume rotational symmetry such as Thomson scattering (Ref 13). Each of the Gaussian profiles is determined by six independent parameters A , b_1 , b_2 , ϕ , x_0 and y_0 (Fig. 8) resulting in 18 variables to reconstruct the obtained section profiles. These parameters allow for ellipsoidal fits even though it has turned out that a circular fit might suffice. To perform an automatic fit, an expectation maximization (EM) algorithm (Ref 14), based on the use of gradients to determine the maxima and minima, is chosen (Ref 15) based on ease of implementation and fast convergence. This way a set of parameters can be found that are most suited to reconstruct the measured section. These parameters represent the global minimum of the EM fit, which is obtained after numerous iterations.

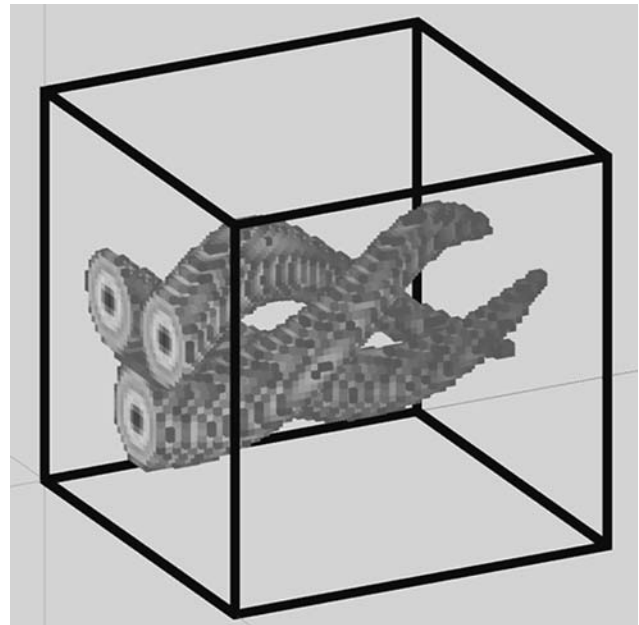


Fig. 9 Result of simulation of complete plasma jet using three Gaussian profiles with exponential decay (z) and vortex component

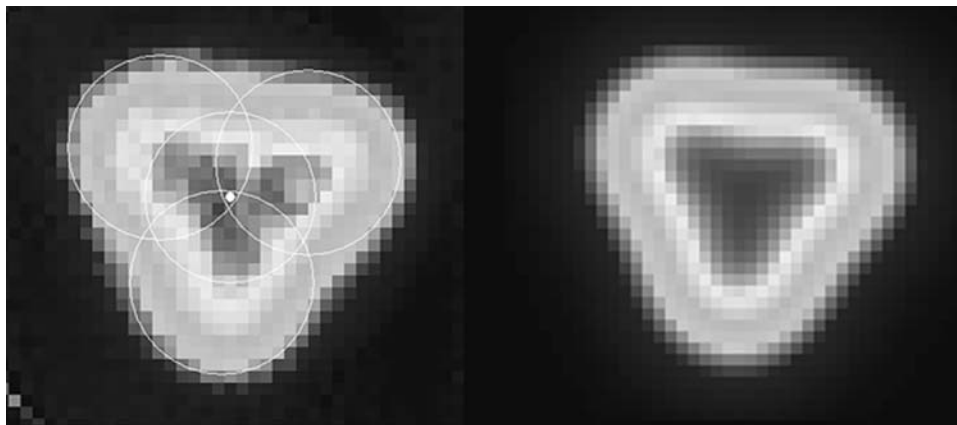
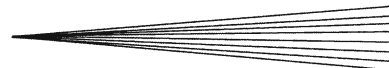


Fig. 10 Comparison of measured (left) and simulated (right) triple-arc plasma jet cross section near the nozzle exit



One example for the results of this algorithm is given in Fig. 9. Using the sum of the three Gaussian profiles implementing the dissipation of the arc jet along the spray direction z through an exponential decay term [$\exp[-(z/z_0)]$], a plasma jet can be simulated. The border of the arc jet is defined by the pixel-to-pixel gradient of the intensity. The current condition is set by comparison with brightness results of experimental data. Adding an azimuthally rotational component, as maybe produced in the Triplex torch by adding a vortex flow, a picture is generated with the same dimensions as the tomography system would deliver. While this image is by no means a realistic representation of a triple-arc system, it demonstrates how possible physical causes for jet behavior can be identified by comparing real measurements with simulated images. First comparisons of measurements and simulations (Fig. 10) in a single plane already demonstrate the potential.

5. Summary

A measurement system for nonrotational symmetric plasma sources has been developed. First experiments using triple-arc plasma torches have shown the potential this diagnostic system may have on the design and operation of new plasma sources. In connection with an adequate simulation tool, tomography may be used to further the understanding of multielectrode systems. More work is needed to benchmark this tool, to evaluate the influence of noise on the reconstruction, and to determine its limitations. Developments are under way to enable real-time tomography by using 60 individual cameras and to determine the jet temperature by performing spectrally resolved measurements.

References

1. Z. Duan and J. Heberlein, Arc Instabilities in a Plasma Spray Torch, *J. Therm. Spray Technol.*, 2002, **11**(1), p 44-51
2. L. Beall, Z. Duan, J. Schein, M. Stachowicz, M.-P. Planche, and J. Heberlein, Controls for Plasma Spraying Based on Plasma Jet Stability Analysis, *Proc. 15th ITSC '98* (Nice, France), Vol. I, ASM International, 1998, pp. 815-820
3. A. Asmann, A. Wank, H. Kim, J. Heberlein, and E. Pfender, Characterization of the Converging Jet Region in a Triple Torch Plasma Reactor, *Plas. Chem. Plas. Proc.*, 2001, **21**(1), p 37-63
4. J. Friedrich, Bemerkungen zur Abelschen Integralrechnung, *Z. Angew. Math. Phys.*, 1960, **11**(3), p 191-197
5. J. Zierhut, P. Haslbeck, K. Landes, G. Barbezat, M. Müller, and M. Schütz, TRIPLEX—An Innovative Three-Cathode Plasma Torch, *Proc. 15th ITSC*, (Nice, France), Vol. 2, ASM International, 1998
6. J. Zierhut, “Entwicklung von Diagnostikverfahren zur Optimierung von Plasmaspritzsystemen (Development of Diagnostic Methods for Optimizing Plasma Spray Systems),” Ph.D. Thesis, Universität der Bundeswehr, Munich, Germany, 2000 (in German)
7. H. Weckmann, A. Syed, Z. Ilhan, and J. Arnold, Development of Porous Anode Layers for the Solid Oxide Fuel Cell by Plasma Spraying, *J. Thermal Spray Technol.*, 2006, **15**(4), p 604-699
8. J. Schein, J. Zierhut, M. Dzulko, G. Forster, and K.D. Landes, Improved Plasma Spray Torch Stability Through Multi-electrode Design, *Contr. Plas. Phys.*, 2007, **47**(7), p 498-504
9. K.D. Landes, G. Forster, J. Zierhut, M. Dzulko, and D. Hawley, Computer Tomography of Plasma Jets—Applied on a TRIPLEX II torch, *Proc. ITSC 2004, Process Diagnostics II* (Osaka, Japan), ASM International, 2004
10. B. Marlow and A. Kraft, “Tomographische Emissionsspektroskopie am thermischen Plasmastrahl (Tomographic Emission Spectroscopy on Thermal Plasma Jets),” Master Thesis, Universität der Bundeswehr, Munich, Germany, 2003 (in German)
11. F. Natterer, The Mathematics of Computerized Tomography, Teubner, Stuttgart, 1986, ISBN 3-519-02103-X, p 102-155
12. G.T. Hermann, Image Reconstruction from Projections, *The Fundamentals of Computerized Tomography*, Academic Press, 1980
13. G. Gregori, J. Schein, P. Schwendinger, U. Kortshagen, J. Heberlein, and E. Pfender, On Thomson Scattering Measurements in Atmospheric Plasma Jets, *Phys. Rev. E*, 1999, **59**(II-B), p 2286-2291
14. A.P. Dempster, N.M. Laird, and D.B. Rubin, Maximum Likelihood from Incomplete Data via the EM Algorithm, *J. R. Stat. Soc. B.*, 1977, **39**, p 1-38
15. C. v. Zombory, “Analytische Nachbildung von Plasmafreistrahprofilen (Analytical Emulation of Plasma Jet Profiles),” Master Thesis, Universität der Bundeswehr, Munich, Germany, 2004